Discrimination of Strombolian eruption types using very long period (VLP) seismic signals and video observations at Mount Erebus, Antarctica

Mah, S. Y.

Department of Earth and Environmental Sciences,

New Mexico Institute of Mining and Technology,

Socorro, New Mexico, USA

Abstract

Strombolian eruptive activity from the open phonolitic lava lake of Mount Erebus generates very long period (VLP) signals with prominent spectral energies at periods of 7, 11, 21, 25 s. These signals have been observed on a seasonal basis in both targeted PASSCAL deployments and, more recently, by permanently installed broadband seismometers. We have also observed lava lake surface activity with a time-stamped crater surveillance video camera. We examined 257 strombolian eruptions at permanent station E1S from December 1999 to October 2002 to assess the consistency of these signals. Generally, the VLP signal, which persists for several minutes following an eruption, is very stable with time and from event to event. However, the initial 5 seconds of signal exhibits significant variations in polarity and timing. We classified VLP signals into 3 families. Group 1 events consist of displacement VLP signals which have initial positive (up) polarity. Group 2 consist of VLP signals with first arrivals of displacement VLP signal having negative (down) polarities. The final type of VLP signals, group 3, shows a large pulse-like overprint with a period near 25 s. Due to the low signal to noise ratios of VLP signals, initial incidence angles show a large variations within groups. However, we note strong a concentration of consistent incidence angles of VLP signals observed from 1999 to the end of 2002. This suggests there is no correlation of initial polarity and the VLP source depth or force system. Events with positive polarity are systematically more emergent than events with negative polarity. Video observation shows positive initial polarity events have a vertical jet-like eruption style, whereas events with negative polarity feature more radial ejecta. The proportion of Group 1 and Group 2 families are temporally variable, and event size gradually decreased over the study period. We conclude that differences in gas slug ascent characteristics are responsible for the differences in initial VLP polarity and character, probably due to at least two distinct gas slug coalescence regions and associated differences in slug ascent characteristics and eruption style.

1 Introduction

Mount Erebus (Figure 1) has exhibited persistent Strombolian activity for at least several decades from a long-lived phonolitic lava lake, and has been sporadically observed for the last 30 years. The lava lake serves as a window into a near-summit magma reservoir. Long-living open lava lake systems are rare and few such systems have been reported. This open conduit system makes detailed video observation possible. Visual and seismo-volcanic monitoring at Mount Erebus shows strombolian eruptions are dominant at the surface of the lava lake. These strombolian eruptions are mainly due to a simple gas slugs which probably form and nucleate in the upper section of the conduit system. Erebus volcano shows a very small quantity of internal earthquakes or volcano-tectonic events.

Seismic monitoring at Mount Erebus began in 1974 using short period seismometers. During the 1980's and early 1990's, US, New Zealand, and Japanese scientists cooperated to operate an analog telemetered network of short-period stations (Rowe and Kienle, 1986; Kaminuma, 1994). Additional volcanic monitoring, including infrasound (Kaminuma et al., 1985) and a surveillance video camera monitoring the lava lake from 1986 to 1990 (Dibble et al., 1994). In 1992, the New Mexico Institute of Mining and Technology (NMIMT) established the Mount Erebus Volcano Observatory (MEVO). Prior to MEVO, six short period seismometers with 1 Hz corner frequency (vertical component Mark Products L4C seismometers) were installed on the

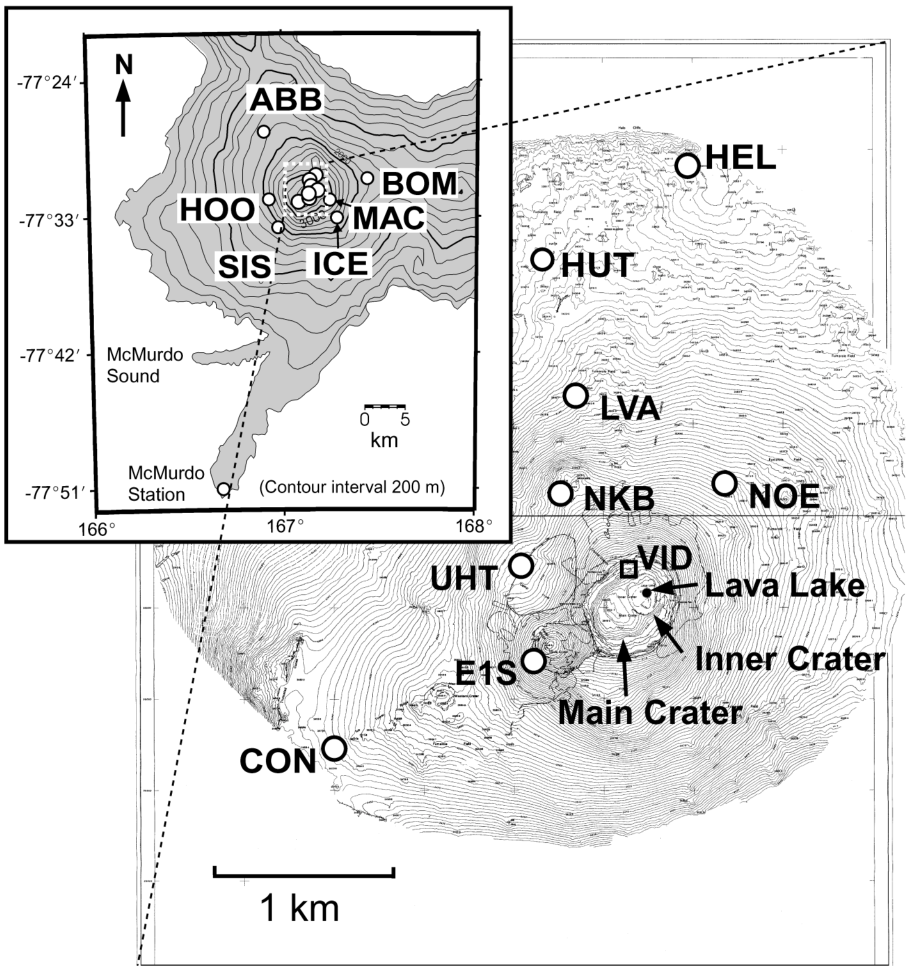

Figure 1. Mount Erebus, showing location of broadband stations installed in the 1999-2000 field season, permanent station E1S, crater surveillance camera site (VID), short period seismometers and Interdisciplinary Surveillance Instrumentation (ISI) sites installed in 2002-2003(Table 1). After Aster et al., 2003a.

flank and summit (Figure 1) regions of the volcano. In subsequent years the MEVO network was expanded to ten stations on the Mount Erebus Volcano (Table 1).

In late 1996 and early 1997, a 2-month pilot deployment of broadband seismic experiment was conducted using three-component Guralap CMG-3ESP broadband seismometers with a low-frequency response corner of 0.03 Hz. These were obtained from the IRIS PASSCAL instrument pool and were deployed in the summit area at the sites HUT, LVA, and NKB (Figure 1; Rowe et al., 1998). In late 1999, a larger temporary network of broadband stations was installed in the summit area at E1S, CON, UHT, NKB, LVA, NOE, HUT, and HEL (Table 1; Aster et al., 2003a). In December 2001, a permanent broadband station was installed at E1S and along with a lava lake surveillance camera. In 2002, additional permanent broadband stations were installed around the summit plateau at CON, HUT, HOO, NKB; a fifth is planned for the crater rim in 2003 (Table 1; Aster et al., 2003b).

VLP signals observed at Mount Erebus are solely associated with Strombolian eruptions (Figure 3). Ash eruption and tremor episodes show no embedded VLP signals. However, the volcanological environments which generate VLP signals globally vary from eruptive to non-eruptive systems and low viscosity to higher viscosity systems. Examples of the eruptive system are Mount Erebus, Antarctica (Rowe et al., 1998, 2000), and Stromboli, Italy (Chouet et al., 2001). Examples of non-eruptive events generating VLP

Station Name	Latitude	Longitude	Elevation	Station Type
ABB	-77.27	166.54	1789	S
BAR	-77.34	166.15	46	S
BOM	-77.30	167.26	2012	S
CON	-77.32	167.05	3453	S, B99, IS
E1S	-77.31	167.08	3708	S, B96, B99, BP, IS
HEL	-77.30	167.10	3368	S, B99
HOO	-77.31	166.55	2121	S, IS
HUT	-77.51	167.14	3320	B96, B99
ICE	-77.33	167.16	2355	S
LEH	-77.51	167.14	3344	IS
LVA	-77.72	167.15	3455	B96, B99
MAC	-77.31	167.14	3337	S
MCM	-77.51	166.40	100	S
NKB	-77.52	167.15	3570	B99, IS
NOE	-77.52	167.16	3557	B99
OBS	-77.51	166.40	100	S
SIS	-77.33	166.58	1800	S
UHT	-77.53	167.14	3561	B99

Table 1. Seismic stations at Mount Erebus. S for short period seismic station, B96 for Broadband seismic experiment of 1996 deployment, B99 for Broadband seismic experiment of 1996 deployment, BP for permanent broadband station at E1S, and IS for 2002-2003 installed integrated seismic stations.

signals include Aso, Japan (Kawakatsu, 1994; Kaneshima et al., 1996) and Popocatepetl, Mexico (Arciniega-Ceballos et al., 1999). The VLP signals generated by such a diverse group of volcanoes suggest that VLP signals probably have several source mechanisms.

The characteristics which identify these VLP signals are as follows: They are commonly most easily visible in the near-field of seismic sources with a rapid geometric spreading factor (e.g. proportional to R^{-2}; Arciniega-Ceballos et al., 1999); the waveforms of VLP signals are highly repeatable (Arciniega-Ceballos et al., 1999; Rowe et al., 1998; Dreier et al., 1994); the onsets of VLP signals where there is an eruption association are always sometime (2-5 seconds) before the surface explosion (Kawakatsu et al., 2000; Neuberg et al., 1994; Rowe et al., 1998; 2000); and the VLP waveforms which accompany surface blasts look like a wave train, but the VLP waveform which accompanies LP and Hybrid events looks like a simple impulse (Arciniega-Ceballos et al., 1999; Hydayat et al., 2000; Nishmura et al., 2000).

Recently, broadband seismometers have been deployed on in several volcanic systems in the study of the VLP signal band. For example, broadband seismic observations have recently been conducted at Stromboli, Italy (Neuberg et al., 1994; Chouet et., 1999; Kirchdölfer, 1999; Weilandt and Forbringer, 1999), Mount Erebus (Rowe et al., 1998; 2000; Aster et al., 2003a), Kilauea, Hawaii (Ohminato et al., 1998; Almendros et al., 2002), Popocatepetl, Mexico (Arciniega-Ceballos et al., 1999), Aso, Japan (Kaneshima et al., 1996; Kawakatsu et al., 2000; Legrand et al., 2000), Merapi, Indonesia (Hydayat et al., 2000, 2003), and Satsuma-Iwojima (Ohminato and Ereditato, 1997). Many features of the VLP source remain enigmatic, but some successful modeling has been accomplished at Stromboli (e.g. Chouet et al., 2003) using mass transport modeling of magma in conduit systems.

2 Broadband Seismic Observation at Mount Erebus, Antarctica

Seismic observation using temporary deployments of broadband seismometers (Guralp CMG-3ESP with corner period 30 s) at Mount Erebus, Antarctica started in November, 1996 - January, 1997. These 1996 deployment data showed very long period signals, where a 21 s spectral peak was the lowest frequency, associated with lava lake Strombolian explosions (Rowe et al., 1998; 2000). MEVO (Mount Erebus Volcanic Observatory) and PASSCAL personnel installed broadband seismometers (30 s Guralp CMG-3ESP and 120 s CMG-3T) and acoustic stations at eight sites on the summit plateau across an azimuth range (relative to the lava lake) of approximately 180 degrees in December, 1999 - January 2000. During the 2001 field season we installed a permanent broadband seismic station (E1S; Guralp 40T with 30 s corner period) and an inner crater surveillance camera. During the 2002-2003 field season, we installed five integrated multidisciplinary stations developed under NSF MRI funding in association with Guralp Systems, featuring infrared, infrasound, broadband seismometry, 2-channel GPS, weather, and system state-of-health data streams. With the addition of sixth planned for station in 2003 featuring HCI and CO2 sensors, this new system will usher in a new era in modern observations of VLP and other phenomena at Erebus while spearheading near instrumentation technologies for general volcano observation (Aster et al., 2003b).

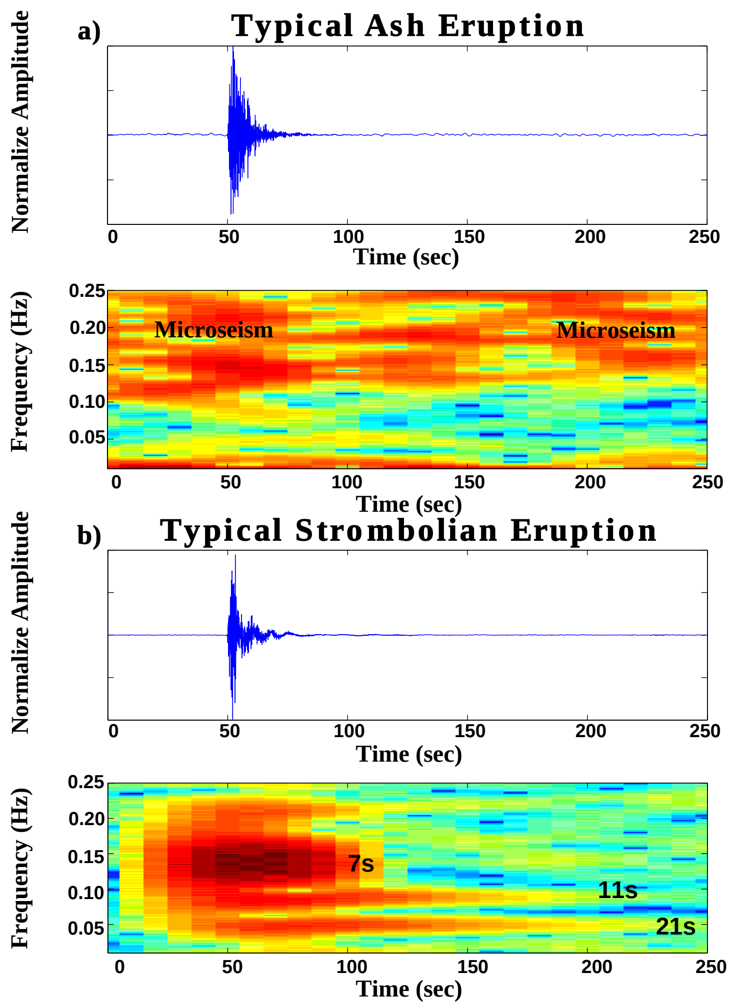

Figure 2. Comparison of Main lava lake event and Ash vent events.This Figure show velocity seismogram and its corresponding low frequency spectrogram. a) ash vent event. This event shows no VLP spectral components on the spectrogram. Due to the oceanic microseism, some energy is visible around 7s, b) Typical strombolian event at Mount Erebus. This event clearly shows characteristic VLP spectral peaks (7s, 11s, and 21s) on the spectrogram.

Broadband displacement seismograms from Erebus Strombolian explosions are dominated by near-field VLP signals, and are highly repeatable from event to event. These observed VLP signals indicate a non-destructive, nearly repeatable source mechanism lasting at least from 1996 to the end of 2002. The 1999 field data show highly similar waveform across the recording network. This suggests these VLP signals are mainly source-dominated and are not strongly affected by their paths. Typical repeatable lava lake strombolian explosions show three dominant spectral peaks (7s, 11s, and 21s). However, ash vent eruptions never show VLP spectral components (Figure 2). In this study, we primarily examine VLP displacement signals which were recorded at E1S station (approximately 700 m from the lava lake).

3 Observations

We analyzed 257 Strombolian eruptions observed at E1S, the station closest to the lava lake and typically with the highest signal to noise ratio. Due to limited battery capacity, during the Antarctic winter, this station stopped recording after mid April 2001, and restarted in January 2002. 90 events were recorded in the 1999 season, and 57 and 110 events were recorded in the 2001 and 2002 seasons, respectively.

We classify displacement VLP signals into 3 major groups based on initial polarity, shape, and spectral content (Figure 3). Group 1 consists of displacement records where VLP signal have positive (up) first arrivals (Figure 3a). Group 2 consists of VLP displacement signals that have negative (down) onsets (Figure 3b). Group 3 events show a simple pulse-like shape (Figure 3c) and are very different from Group 1 or 2 events (Figure 3). We observed only 4 events for group 3; however, these events were unique in their unusual pulse-like shape and frequency contents. Group 1,2, and 3 events show clear seismo-acoustic wave arrivals which are characteristic of Strombolian eruptions (Figure 4). However weather conditions and camera downtime unfortunately did not permit us to obtain video records associated with the Group 3 eruptions. Figure 5 shows a stacked seismogram of each group and corresponding power spectra for Up (Group 1), Down (Group 2), and Pulse shape (Group 3), respectively. The frequency spectrum show the characteristic 21 s, 11 s, and 7 s spectral peaks for both of the positive (Group 1) and

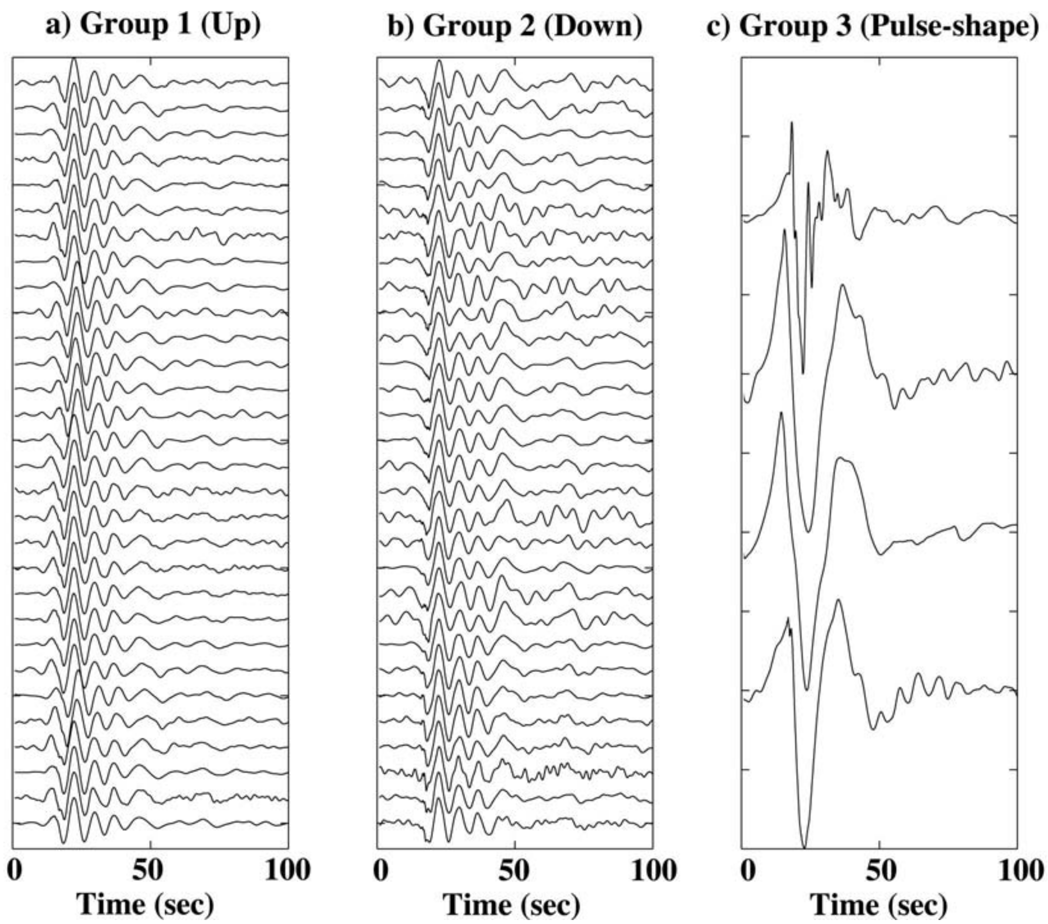

Figure 3. Vertical component displacement seismograms of each event family. a) Group 1 (positive first VLP onsets), b) Group 2 (negative first VLP onsets), and c) Group 3 (pulse-like shape).

negative (Group 2) polarity groups (Rowe et al., 1998, 2000; Aster et al., 2003a, b). But the frequency content for the Group 3 pulse-shape stacked seismograms includes only spectral peak, around 25 s.

Group 1 and Group 2 have high wave-form similarity except for the first arrival polarity and earliest wave form of the VLP signals (Figure 4). To evaluate general characteristics of Group 1 and Group 2 events, we stacked the events of each group (131 events for Group 2 and 113 events for Group 1). The first 5 seconds of VLP onsets show large variations; however, they are two groups have nearly the same displacement in the VLP coda (Figure 6). This suggests that VLP source mechanisms are dominated by the same processes aside from the first onset (approximately the initial 5 s).

Strombolian eruptions were recorded by a surveillance camera located approximately 350 m from the lava lake (Aster et al., 2003b). In clear weather conditions, the camera reveals interesting source features for down (Group 2) and up (Group 1) first onset events. Figure 7 shows positive first onset VLP signal observed from E1S station located approximately 700m from the lava lake and corresponding video frames, cut to 1 second intervals. The first frame shows no lava lake surface activity. However, the second and third frames show vertical jet-like eruption motion. The remaining frames (4, 5, 6) show no comparably diagnostic features. On the other hand, Figure 8 shows an eruption with negative first onset polarity and corresponding video frames. This Figure shows different eruption aspects from Figure 7. The

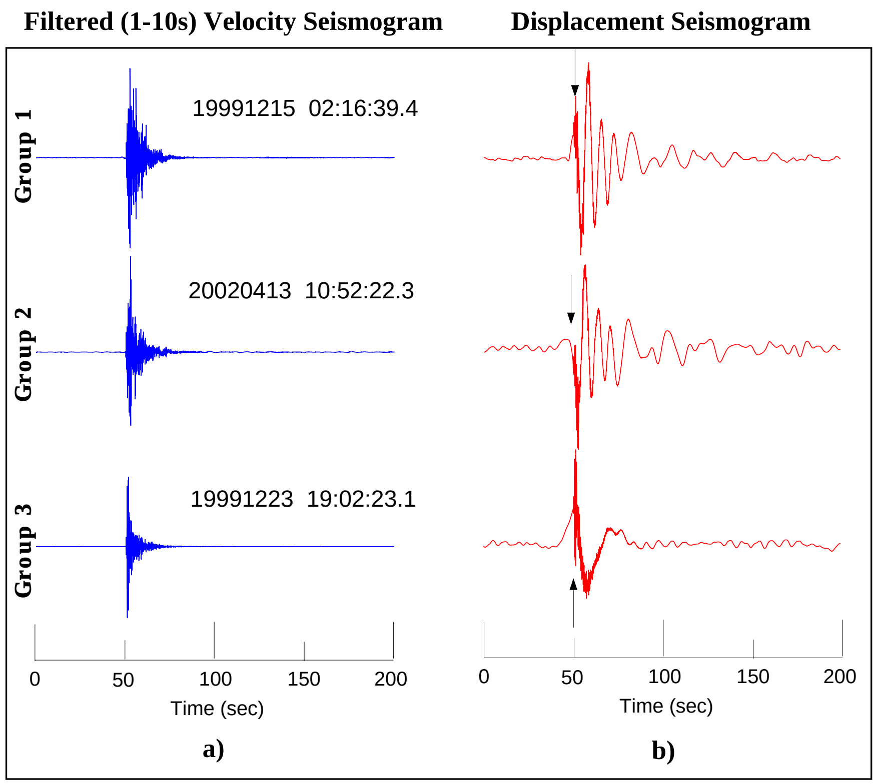

Figure 4. Seismo-acoustic signals of each family. Each family shows clear onset of seismo-acoustics wave from eruption activity (arrows).

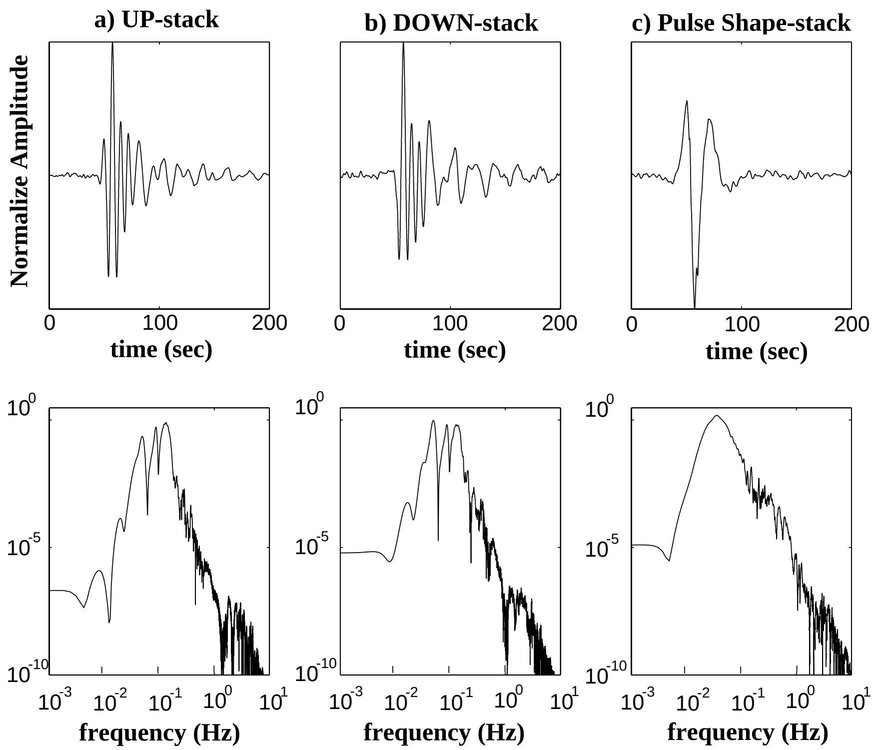

Figure 5. Stacked seismograms of each group and corresponding power spectrum. a) Up-motion stacked seismogram and the corresponding power spectrum (Group 1), b) Down-motion (Group 2), c) Pulse-shape (Group 3).

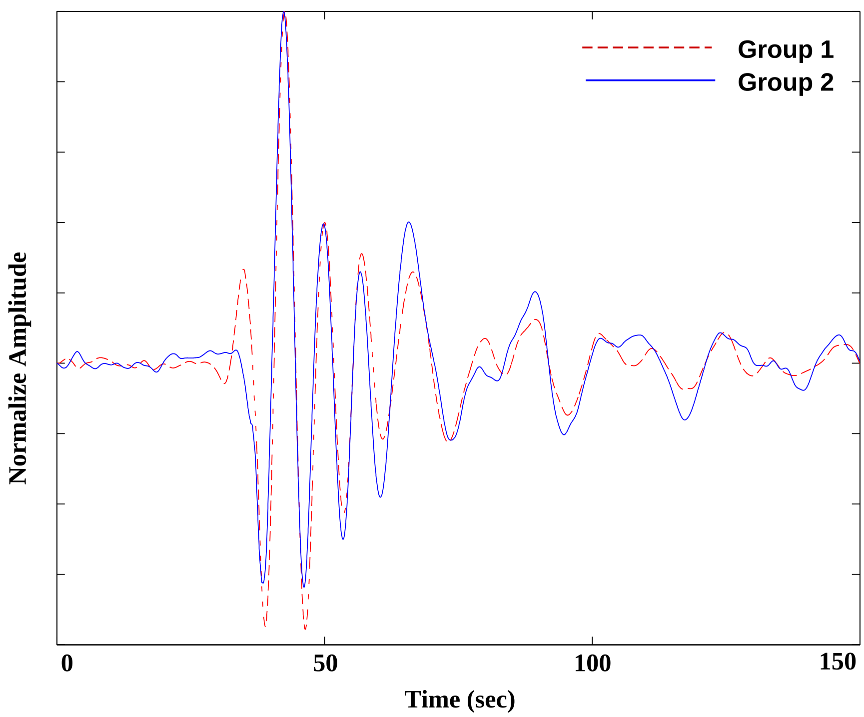

Figure 6. Stacked vertical component of the displacement seismograms of Group 1 (positive first onset; stacked 131 events) and Group 2 (negative first onset; stacked 113 events).

first frame shows no activity at the lava lake surface. However, in the second frame, the lava lake surface starts to inflate, and the third frame shows the exploding lava lake surface. The rest of video frames show more radial ejecta than Figure 7. We note that the lava lake surface phenomena and broad-band displacement seismogram are not in phase. This indicates that the VLP displacement source is not caused by a lava lake surface activity. The source of VLP signals is thus located beneath the lava lake surface. Unfortunately, again, we have not yet observed Group 3 (simple-pulse shape events) with the inner crater surveillance camera.

Strombolian eruption activity observed with broadband seismometers at Mount Erebus dramatically decreased from the 1999 field season to the 2002 season. During the 1999 field season, eruption activity averaged about 2 eruptions per day, but in the 2001 season, explosive activity averaged about 1 explosion per two days. This trend continued through 2002. In 2002, eruption activity averaged 1 explosion per three days (Figure 9a). This tendency was also observed in short-period seismometer records (Figure 9c). Differences in the number of events between short-period and broad-band observation may be caused by icequakes, falling rocks, etc. The eruption size also gradually decreased from 1999 to 2002 (Figure 9b) and eruption activity has decreased to near zero during the first part of 2003. Interestingly, this decreasing strombolian activity has been accompanied by a dramatic increase in (previously rare) harmonic and non-harmonic tremor (M. Ruiz, pers. commun.).

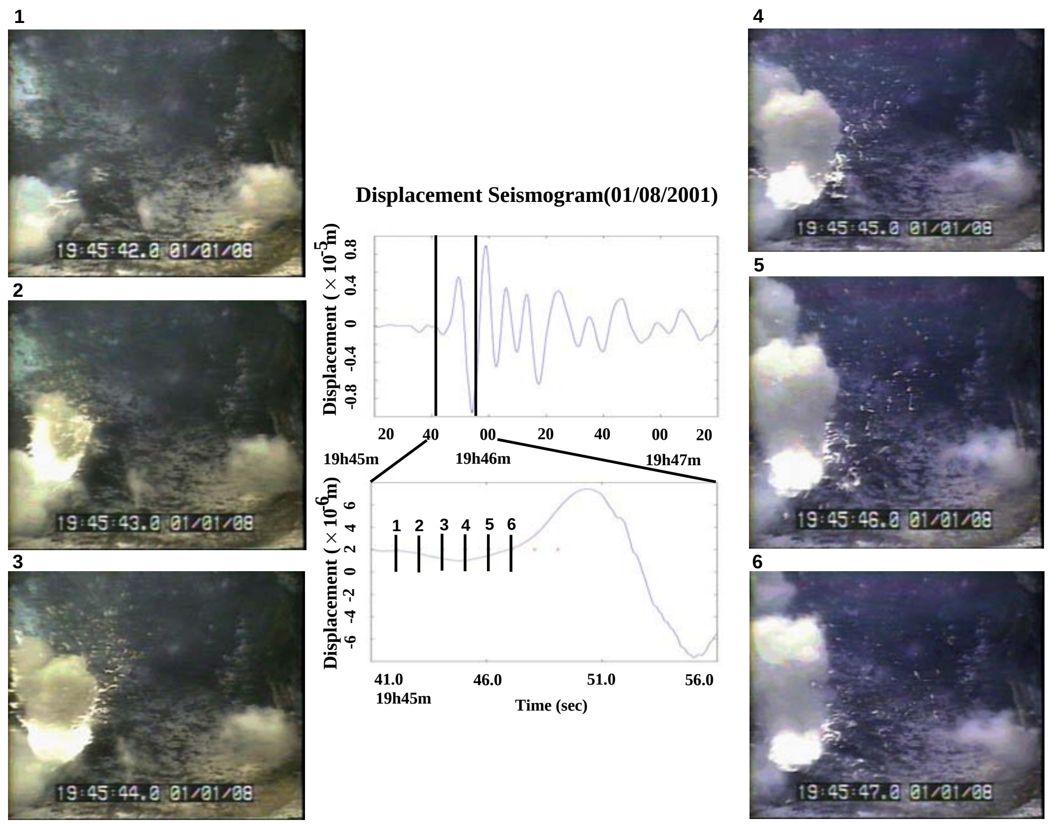

Figure 7. Vertical component displacement seismogram and the corresponding video frames. This Figure shows positive VLP onset and specific eruption sequences.

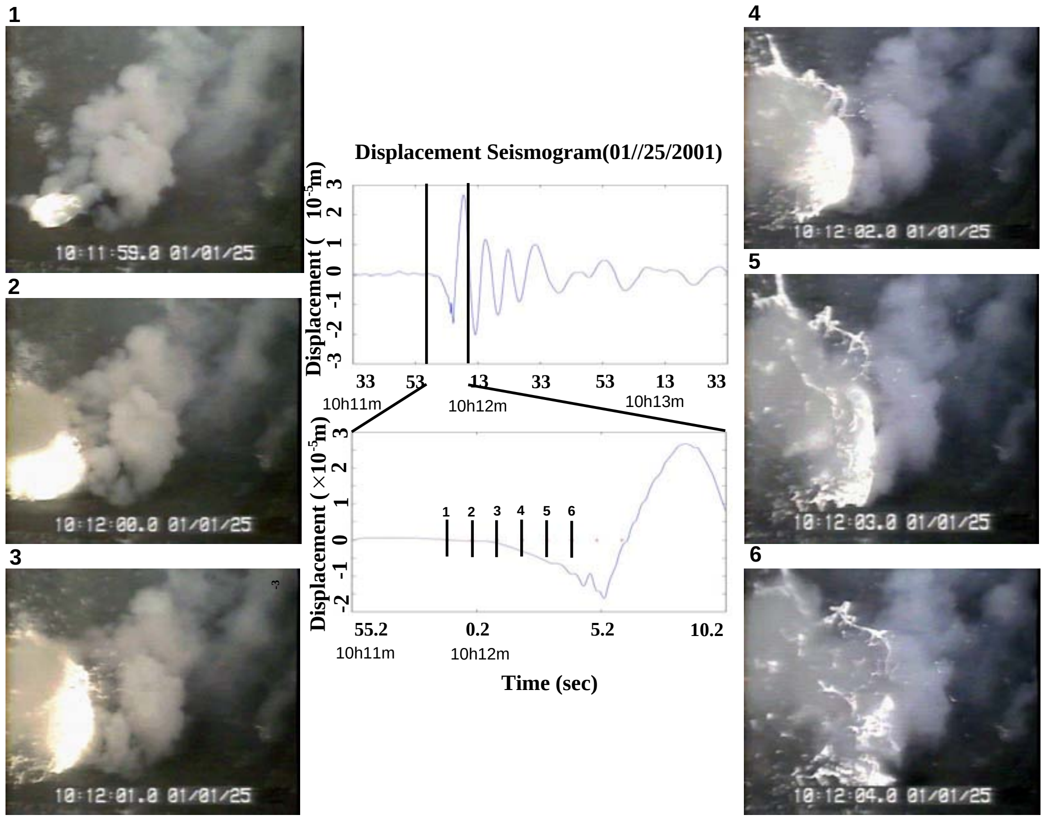

Figure 8. Vertical component displacement seismogram and the corresponding video frames. This Figure shows negative VLP onset and specific eruption sequences.

VLP displacement records, aside from initial polarity, are very consistent from event to event. This suggests a non-destructive source process (Rowe et al., 1998; Aster et al., 2003a). As opposed to the high repeatability and VLP coda signals, pre-eruptive VLP signals show a wide variety of timing and polarity. We note that the first onsets of vertical component displacement observed in the 1999 field season are dominantly positive polarities. However, the tendency of positive polarity dominance changed gradually from the 1999 to the 2002 field season (Figure 9a). For 1999, most of the vertical component VLP signal is first onset polarity is positive polarity. However, in 2002, first onset polarities are dominantly negative polarities. Due to the event size decrease, in 2002, we observed many unclear first onset events. We also investigated apparent incidence angles of initial 5s VLP signals using particle motion analysis. The results of particle motion analysis show very stable incidence angles from the 1999 to the 2002 field data. Although 2002 data show some variations of incidence angle compared to the 1999 and the 2001, most energy rays are concentrated in almost the same range as 1999 and 2002(Figure 10). This argues for a consistent VLP source location and force system during this period.

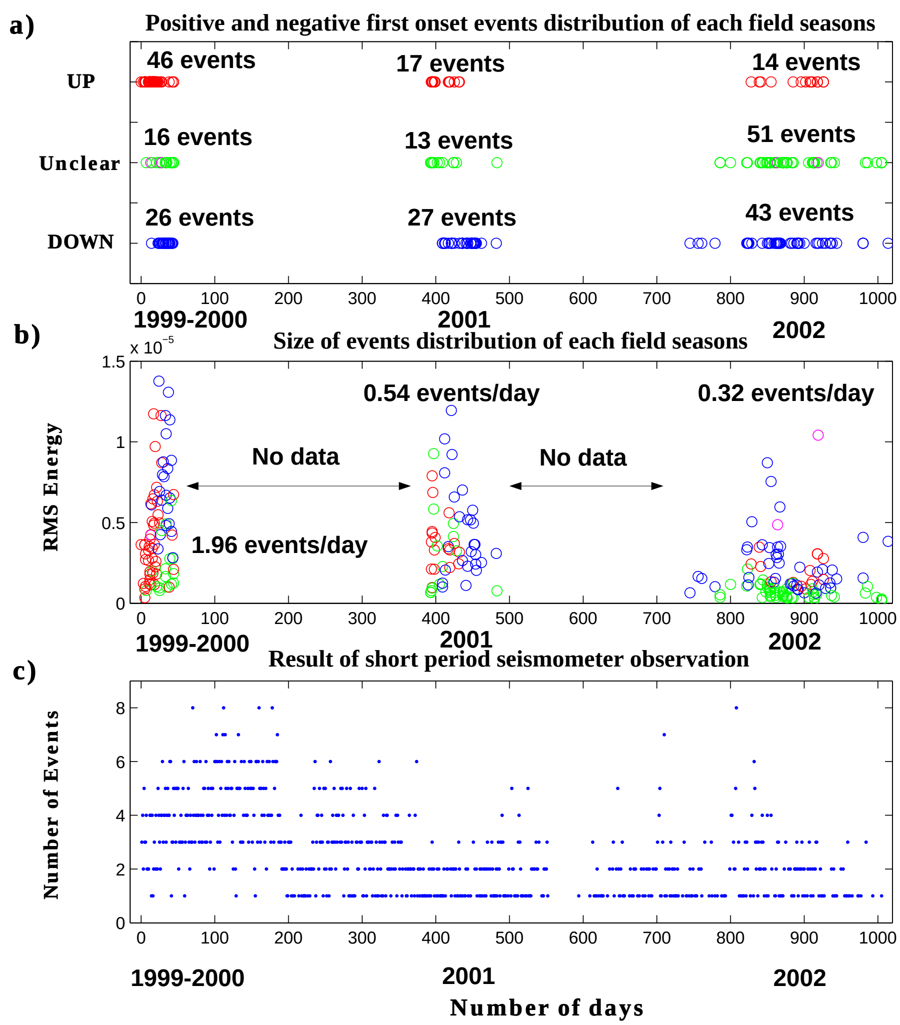

Figure 9. Seasonal distribution of first onset polarities and event sizes (from Dec. 10, 1999 to Oct. 01, 2002. a) Up- and Down- motion first onset distributions of each field season, b) Event size distributions, c) Result of short period seismometer observation. Red circles represent Group 1 events, blue circles represent Group 2 events, pink circles represent Group 3 events, and green circles represent unclear first VLP onsets.

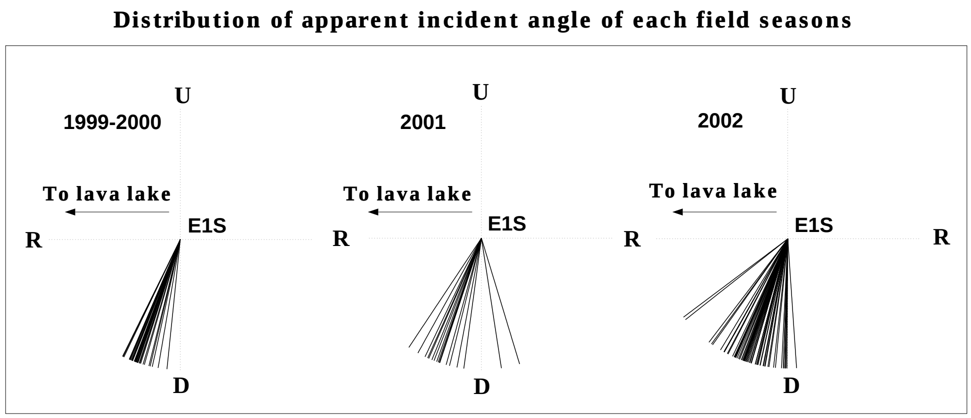

Figure 10. Seasonal distribution of apparent incident angle, 1999-2000, 2001, 2002 field season.

4 Discussion

Recently, broadband near-field seismic observations of VLP signals have been applied to begin to reveal source features (Chouet et al., 2003), and recent broadband observations have shown that the VLP signals occur in both erupting systems and non-erupting systems. In this study we did not determine source depth precisely, due to the one station (E1S) limitation and the complications of accurately modeling near-field displacements on volcanoes. However, the apparent incidence angles and VLP coda signal of each field season are very stable (Figure 10). These results suggest that, regardless of first onset polarities, the source locations, mechanisms, and Group 1 and Group 2 VLP coda signals are in almost identical. Several researchers reported Strombolian eruptions had very shallow source depths. For example, Chouet et al.(1999) studied VLP signal source depth at Stromboli Volcano and determined a depth of 300 meters beneath the active vents; Kirchdöfer (1999) determined a source depth between 50 and 200m below the crater terrace at Stromboli Volcano; Hydayat et al. (2000) reported a source depth of VLP signal at 100m below the summit dome of Merapi Volcano, Indonesia. Due to the absence of a sufficiently detailed elastic model, many researchers used particle motion analysis to estimate source location. Particle motion analysis will work if the seismic source is purely dilatational, if near-field source effects do not complicate the particle motions, and if the influence of layering and other structural and topographic complications can be neglected.

Events similar to our Group 3 are observed at Merapi, Indonesia (Hydayat et al., 2000; 2002; 2003), and Kilauea, Hawaii (Almendros et al., 2002). Hidayat et al. (2000; 2002; 2003) interpreted that simple pulse shape as a surface tilt effect caused by inflation and deflation of the volcano. Almendros et al. (2002) analyzed a pulse shape VLP signal source with a location 8 km below Kilauea caldera and interpreted it as a response of plumbing system inside the volcano. Group 3 type events are only observed at non-erupting systems; however, our simple pulse type events are clearly associated with the Strombolian eruptions (Figure 4).

Video observations show that Group 1 positive polarity events have a vertical jet-like eruption style, and Group 2 negative polarity events have considerably more radial ejecta. Combining video and VLP observations, we conclude that the early VLP signal differences between Group 1 and Group 2 events are due to differences in gas slug ascension. The ascending speed of gas slugs and the corresponding forces applied to the conduit system will depend on the pressure differences between inside the gas bubble and the surrounding lava, the viscosity of lava, the shape of the volcano conduit wall, and the shape of the gas bubble. The source mechanism of VLP signals is not clear, however, Aster et al. (2003a) examined several possible source mechanisms for VLP signal generation inside the Erebus conduit system and concluded that the initial variable signal was due to the gas slugs ascent whereas the repeatable coda was due to lava lake recharge forces possibly interacting with a shallow resonator. Ohminato et al. (1998) and Legrand et al. (2000) examined moment tensor solution to a non-eruptive VLP system (Kilauea, Hawaii) and an eruptive system (Aso Japan), respectively. Ohminato et al. (1998) used 9 component moment tensor elements that included 3 components of isotropic force, 3 components of deviatoric force, and 3 single forces (Kilauea, Hawaii). Legrand et al. (2000) used 6 component moment tensor elements that included 3 components of isotropic force and 3 components of deviatoric force. They found a mainly isotropic expansion and small portion of deviatoric force which was best explained by vertical crack opening. However, Ohminato et al. (1998) found a subhorizontal crack opening with negligible single forces at Kilauea. Chouet et al. (2003) used 9 elements of moment tensor which used the inversion method of Ohminato et al. (1998). Chouet et al. (2003) obtain relatively large single force (10^8 N) and volumetric source components. Kanamori et al. (1984) investigated seismic body wave excitation and proposed a significant vertical single force of the Mount St. Helens' eruption of May 18, 1980. Although Mount St. Helens eruption had a very large magnitude, the concept of vertical single force may apply to other erupting systems. As discussed by Aster et al. (2003a), VLP signal generation inside the volcano may combine several mechanisms (single force, oscillatory recharge, isotropic expansion, etc).

Determining the nature of VLP signals requires numerous broadband instruments. At Mount Erebus, we installed a permanent broadband seismic station at ElS (approximately 700 m from the lava lake). Four additional broadband stations with multiple sensors were installed through the 2002-2003 field season. We hope that this long-term broadband seismic recording will reveal more characteristics of VLP source features as eruption activity at Erebus continuous to evolve.

5 Conclusions

Mount Erebus volcano generates 3 types of VLP signals, all associated with Strombolian eruptions. The first kind of VLP signal has explosive first onsets, the second kind has implosive first onsets and the third kind is a simple pulse-shape. Although first motions of VLP signals show significant variations, the extended (several minutes) VLP coda is quite stable in the frequency and time domains. Spectral content is almost the same between Up- (Group1) and Down-motion (Group 2) groups, but not for the third pulse-shaped group (Group 3). Generally, the VLP signals observed at Mount Erebus have 3 spectral peaks at periods of 7 s, 11 s, and 21 s, but Group 3 events have only a single spectral peak (around 25 s). The investigation of variation in VLP incident angles shows no significant variations, which suggests the source region of the VLP signals is almost identical and the first onset polarities of VLP signals do not indicate different VLP source locations. Video observation shows that all positive polarity onset events have subvertical jet-like ejecta, while all negative polarity onset events show for more radial ejecta. Our interpretation of differences between positive and negative first onsets of VLP signals are an indication of variability in slug ascent characteristics. This would introduce variability into the early portion of the source moment tensor and/or the source time function. The proportion of positive and negative type VLP events is temporally variable, and event size has gradually decreased over the past few field seasons as the summit magmatic system continuous to evolve.

6 Acknowledgments

We thank UNAVCO and the IRIS PASSCAL Instrument Center at NMT for essential instrumentation and field assistance. Transportation in Antarctica was provided by the Royal New Zealand Air Force and Petroleum Helicopters incorporated. We also thank the many Raytheon Polar Services individuals and groups at McMurdo for crucial support, including Jesse Crain, Karen Joyce, Sarah Krall, Robbie Liben, MikeMcClanahan, William Nesbit, Richard "Chino" Perales, Robbie Score, Pat Smith, Seth White, and Andy Young. Earthworm assistance was provided by Barbara Bogaert and Alex Bittenbinder of USGS. The gencompress algorithm in Earthworm data transfer is used with permission of Boulder Real Time Technologies. Review comments by Sara McNamara, Phil Kyle, John Schlue, and Richard Aster contributed significantly to the manuscripts. This research supported by NSF Grants OPP-9814291 and OPP-0116577.

References

[1] Almendros J., B. Chouet, P. Dawson, and T. Bond, Identifying elements of the plumbing system beneath Kilauea Volcano, Hawaii, from the source locations of very-long-period signals, Geophys. J. Int. 148, 303-312, 2002.

[2] Arciniega-Ceballos, A., B. Chouet, and P. Dawson, Very long-period signals associated with vulcanian explosions at Popocatepetl volcano, Mexico, Geophys. Res. Lett. 26, 3013-3016, 1999.

[3] Aster R., S. Mah, P. Kyle, W. McIntosh, N. Dunbar, J. Johnson, M. Ruiz, and S. McNamara, Very long period oscillations of Mount Erebus volcano, J. Geophys. Res., in Press, 2003a.

[4] Aster, R., B. Bartel, N. Dunbar, R. Esser, B. Johns, J. Johnson, R. Karstens, C. Kurnik, P. Kyle, M. McGowan, W. McIntosh, S. McNamara, C. Meertens, B. Pauly, M. Richmond, and M. Ruiz, New instrumentation Delivers Multidisciplinary Real-time Data from Mount Erebus, Antarctica, EOS trans. AGU., in review, 2003b.

[5] Chouet, B., G. Saccorotti, P. Dawson, M. Martini, R. Scarpa, G. De Luca, G. Milana, and M. Cattaneo, Broadband measurements of the sources of explosions at Stromboli volcano, Italy, Geophys. Res. Lett. 26, 1937-1940, 1999.

[6] Chouet, B., P. Dawson, T. Ohminato, M. Martini, G. Saccorotti, F. Guidicepietro, G. De Luca, G. Milana, and R. Scarpa, Source mech-

anism of explosions at Stromboli Volcano, Italy, determined from moment tensor inversion of VLP data, J. Geophys. Res., 108(B1), 2019, doi:10.1029/2002JB001919, 2003.

[7] Dibble, R. R., Velocity modeling in the erupting magma column of Mount Erebus, Antarctica, In: Kyle, P. R. (Ed.), Volcanological and Environmental Studies of Mount Erebus, Antarctica, Antarctic Research Series, American Geophysical Union, Washington DC, 17-33, 1994.

[8] Dreier, R., R. Widmer, R. Schick, and W. Zürn, Stacking of broad-band seismograms of shocks at Stromboli, Acta Vulcano. 5, 165-172, 1994.

[9] Hidayat, D., B. Voight, C. Langston, A. Ratdomoputbo, and C. Ebeling, Broadband seismic experiment at Merapi Volcano, Java, Indonesia: very-long-period pulses embedded in multiphase earthquake, J. Vol. Geotherm. Res. 100, 215-231, 2000.

[10] Hidayat, D., B. Chouet, B. Voight, P. Dawson, and A. Ratdomopurbo, Source mechanism of very-long-period signals accompanying dome growth activity at Merapi volcano, Indonesia, Geiphys. Res. Lett., 29(23), 2118, doi:10.1029/2002GL015013,2002.

[11] Hidayat, D. B. Chouet, B. Voight, P. Dawson, and A. Ratdomopurbo, Correction to "Source mechanism of very-long-period signals accompanying dome growth activity at Merapi volcano, Indonesia", Geophys. Res. Lett., 30(10), 1502, doi:10.1029/2003GL017211.

[12] Kaminuma, K., The seismic activity of Mount Erebus in 1981-1990. In: Kyle, P. R. (Ed.), Volcanological and Environmental Studies of Mount Erebus, Antarctica. Antarctic Research Series, American Geophysical Union, Washington DC, 35-50, 1994.

[13] Kaminuma, K., S. Ueki, and J. Kienle, Volcanic earthquake swarms at Mt. Erebus, Antarctica, Tectonophysics 114, 357-369, 1985.

[14] Kanamori, H., J. W. Given, and T. Lay, Analysis of Seismic Body Waves Excited by the Mount St. Helens Eruption of May 18, 1980, J. Geophys. Res. 89(3), 1856-1866, 1984.

[15] Kaneshima, S., H. Kawakatsu, H. Matsubayashi, Y. Sudo, T. Tsutsui, T. Ohminato, H. Ito, K. Uhira, H. Yamasato, J. Oikawa, M. Takeo, and T. Iidaka, Mechanism of phreatic eruptions at Aso volcano inferred from near-field broadband seismic observations, Science 273, 642-645, 1996.

[16] Kawakatsu, H., S. Kaneshima, H. Matsubayashi, T. Ohminato, Y. Sudo, Y. Tsutsui, K. Uhira, H. Yamasato, H. Ito, and D. Legrand, Aso94: Aso seismic observation with broadband instruments, J. Vol. Geotherm. Res. 101, 129-154, 2000.

[17] Kawakatsu, H., T. Ohminato, H. Ito, Y. Kuwahara, T. Kato, K. Tsuruga, S. Honda, and K. Yonogida, Broadband seismic observation at the Sakurajima Volcano, Japan, Geophys. Res. Lett. 19, 1959-1962, 1992.

[18] Kirchdöfer, M., Analysis and quasi static FE modeling of long period impulsive events associated with explosions at Stromboli volcano (Italy), Ann. Geofis. 42, 379-390, 1999.

[19] Kyle, P. R. (Ed.), Volcanological and Environmental Studies of Mount Erebus, Antarctica, Antarctic Research Series, American Geophysical Union, Washington DC, 1994.

[20] Legrand, D., S. Kaneshima, and H. Kawakatsu, Moment tensor analysis of near-field broadband waveforms observed at Aso volcano, Japan, J. Vol. Geothem. Res. 101, 155-269, 2000.

[21] Neuberg, J., R. Luckett, M. Ripepe, and T. Braun, Highlight from seismic broadband array on Stomboli volcano, Geophys. Res. Lett. 21, 749-752, 1994.

[22] Neuberg. J. and T. Pointer, Effects of volcano topography on seismic broad-band waveforms, Geophys. J. Int. 143, 239-248.

[23] Nishimura, T., H. Nakamichi, S. Tanaka, M. Sato, T. Kobayashi, S. Ueki, H. Hamaguchi, M. Ohtake, and H. Sato, Source process of very long period seismic events associated with the 1998 activity of Iwate Volcano, Northeastern Japan, J. Geophys. Res. 105(B8), 19135-19147, 2000.

[24] Ohminato, T., and D. Ereditato, Broadband seismic observations at Satsuma-Iwojima volcano, Japan, Geophys. Res. Lett. 24, 2845-2848, 1997.

[25] Ohminato, T., B. Chouet, P. Dawson, and S. Kedar, Waveform inversion of very long period impulsive signals associated with magmatic injection beneath Kilauea volcano, Hawaii, J. Geophys. Res. 103, 23839-23862, 1998.

[26] Rowe, C., and J. Kienle, Seismicity in the vicinity of Ross Island, Antarctica, J. Geodyn. 6, 375-385, 1986.

[27] Rowe, C., R. Aster, P. Kyle, J. Schlue, and R. Dibble, Broadband recording of Strombolian explosions and associated very-long-period seismic signals on Mount Erebus volcano, Ross Island, Antarctica, Geophys. Res. Lett. 25, 2297-2300, 1998.

[28] Rowe, C., R. Aster, P. Kyle, R. Dibble, and J. Schlue, Seismic and acoustic observations at Mount Erebus Volcano, Ross Island, Antarctica, 1994-1998, J. of Vol. Geotherm. Res. 101, 105-128, 2000.

[29] Wielandt, E., and T. Forbringer, Near-field seismic displacement and tilt associated with the explosive activity of Stromboli, Ann. Geofis. 42, 407-416, 1999.

A Appendix

A.1 Catalog of Events Recorded at E1S and Used in This Study

No	Date	Arrival Time	Max.Amp.(M)	Group
1	19991210	23:48:04.27	5.22e-15	Group 1
2	19991213	14:21:42.99	1.74e-15	Group 1
3	19991215	02:16:39.42	4.90e-15	Group 1
4	19991215	13:40:45.16	6.44e-16	Group 1
5	19991215	18:43:09.05	1.36e-15	Group 1
6	19991215	02:16:39.49	4.90e-15	Group 1
7	19991216	05:26:46.00	1.58e-15	Group 1
8	19991216	06:34:51.19	3.80e-15	Group 1
9	19991216	21:25:37.39	4.19e-15	Group 1
10	19991217	22:35:58.84	1.29e-15	-
11	19991220	04:07:25.57	4.71e-15	Group 1
12	19991220	04:50:02.81	3.81e-15	Group 1
13	19991221	03:24:50.33	1.64e-15	Group 1
14	19991221	07:38:27.34	4.79e-15	Group 1
15	19991222	02:31:21.92	5.88-15	Group 1
16	19991222	12:00:27.91	2.24e-15	Group 1
17	19991222	15:25:59.39	2.67e-15	Group 1

continued on next page

Table 2. *Continued*

No	Date	Arrival Time	Max.Amp.(M)	Group
18	19991222	18:16:59.10	2.60e-15	Group 1
19	19991223	01:24:04.72	1.83e-15	Group 1
20	19991223	04:55:31.78	5.75e-15	Group 1
21	19991223	10:40:15.22	8.52e-15	Group 1
22	19991223	19:02:23.12	5.49e-15	Group 3
23	19991224	11:53:45.24	8.70e-15	Group 2
24	19991225	00:35:10.69	3.02e-15	-
25	19991225	06:52:51.83	4.83e-15	Group 1
26	19991225	16:55:19.59	7.09e-15	Group 1
27	19991225	20:46:58.86	4.18e-15	Group 1
28	19991226	06:54:10.10	2.64e-15	Group 1
29	19991226	14:48:24.23	9.20e-15	Group 1
30	19991227	13:07:06.39	1.65e-14	Group 1
31	19991227	02:19:44.00	7.05e-15	Group 1
32	19991228	00:33:57.31	9.63e-15	Group 1
33	19991228	08:04:23.94	1.59e-15	Group 1
34	19991228	15:30:23.85	5.41e-15	Group 1
35	19991228	18:26:08.10	7.15e-15	Group 1
36	19991229	16:46:26.38	3.57e-15	Group 1
37	19991229	21:23:04.72	1.40e-14	Group 1

continued on next page

Table 2. *Continued*

No	Date	Arrival Time	Max.Amp.(M)	Group
38	19991230	18:36:05.79	3.69e-15	Group 1
39	19991231	12:25:27.14	2.66e-15	Group 1
40	19991231	22:41:55.95	1.35e-15	-
41	19991231	15:23:40.81	1.01e-14	Group 1
42	20000101	12:50:10.92	9.04e-15	Group 1
43	20000102	01:46:04.48	5.46e-15	Group 2
44	20000102	18:27:42.37	7.75e-15	Group 1
45	20000103	07:24:50.63	2.35e-14	Group 2
46	20000104	09:37:01.70	1.18e-14	Group 2
47	20000104	22:41:31.14	1.07e-15	-
48	20000104	23:05:30.67	1.31e-15	-
49	20000104	23:23:28.18	7.64e-15	Group 1
50	20000105	11:03:59.17	7.03e-15	Group 2
51	20000106	02:42:20.88	1.75e-14	Group 1
52	20000107	02:27:55.88	7.01e-15	-
53	20000107	04:00:25.82	1.30e-14	Group 1
54	20000107	09:47:56.05	1.10e-14	Group 2
55	20000107	16:03:11.35	2.93e-14	Group 3
56	20000108	00:48:08.49	1.21e-14	Group 2
57	20000108	15:24:25.86	2.80e-14	Group 2

continued on next page

Table 2. *Continued*

No	Date	Arrival Time	Max.Amp.(M)	Group
58	20000109	04:05:40.44	1.48e-14	Group 2
59	20000109	15:49:50.88	3.02e-14	Group 2
60	20000110	04:46:04.11	1.25e-14	Group 2
61	20000110	19:33:59.67	2.35e-14	Group 2
62	20000112	01:11:50.82	2.73e-15	-
63	20000112	04:03:05.66	1.83e-14	Group 2
64	20000112	13:36:55.13	3.48e-15	-
65	20000113	06:06:31.41	1.62e-14	Group 2
66	20000113	11:12:42.97	9.69e-15	Group 2
67	20000113	20:18:01.24	8.03e-15	Group 2
68	20000113	23:18:56.25	7.24e-15	-
69	20000114	19:10:56.70	1.86e-15	-
70	20000115	00:33:48.67	1.31e-14	Group 2
71	20000115	14:12:20.05	1.00e-14	Group 2
72	20000115	22:17:00.66	2.69e-14	Group 2
73	20000116	22:34:00.69	2.06e-14	Group 2
74	20000117	23:36:30.33	8.27e-15	Group 2
75	20000117	10:40:56.34	1.57e-15	Group 1
76	20000118	00:06:46.01	1.78e-14	Group 2
77	20000118	16:45:30.37	4.67e-15	-

continued on next page

Table 2. *Continued*

No	Date	Arrival Time	Max.Amp.(M)	Group
78	20000118	23:54:32.61	1.04e-14	Group 2
79	20000120	07:05:14.86	1.92e-15	-
80	20000120	08:21:09.18	9.57e-15	-
81	20000120	11:52:00.40	7.42e-15	Group 2
82	20000120	16:20:52.06	1.41e-14	Group 2
83	20000121	07:13:00.36	7.20e-15	Group 1
84	20000121	12:33:33.58	2.95e-14	Group 2
85	20000122	04:28:09.29	4.64e-15	-
86	20000122	14:37:39.56	4.74e-15	Group 2
87	20000123	00:59:30.81	2.19e-15	-
88	20000123	02:07:37.17	1.91e-15	-
89	20000123	03:01:31.92	3.05e-15	Group 1
90	20000123	11:50:04.18	1.01e-14	Group 1
91	20010106	03:27:47.30	1.03e-15	-
92	20010106	16:05:21.99	1.04e-15	-
93	20010107	03:46:38.33	1.05e-15	-
94	20010107	08:02:08.92	5.29e-15	Group 1
95	20010107	21:34:14.67	3.04e-15	Group 1
96	20010108	02:45:09.37	1.15e-15	Group 1
97	20010108	14:04:58.47	1.24e-15	-

continued on next page

Table 2. *Continued*

No	Date	Arrival Time	Max.Amp.(M)	Group
98	20010108	16:47:04.66	1.08e-14	Group 1
99	20010108	19:45:43.88	5.45e-15	Group 1
100	20010108	21:18:10.98	6.10e-15	Group 1
101	20010109	06:53:52.67	9.61e-15	Group 1
102	20010110	04:25:33.71	9.24e-15	-
103	20010110	17:27:01.95	1.46e-14	-
104	20010111	11:13:24.43	4.75e-15	Group 1
105	20010111	21:11:29.18	2.88e-15	Group 1
106	20010112	14:00:05.02	5.84e-15	Group 1
107	20010115	06:35:43.92	5.00e-15	-
108	20010118	21:13:37.93	1.65e-15	-
109	20010122	02:42:27.93	3.24e-15	-
110	20010122	22:31:01.69	2.06e-15	Group 2
111	20010122	23:25:18.77	1.55e-15	Group 2
112	20010125	00:49:21.80	1.19e-14	Group 2
113	20010125	10:12:00.15	1.51e-14	Group 2
114	20010126	22:35:03.62	3.43e-15	Group 2
115	20010130	05:04:56.07	5.04e-15	Group 1
116	20010130	21:07:35.27	5.32e-15	Group 2
117	20010131	16:38:58.82	8.64e-15	Group 1

continued on next page

Table 2. *Continued*

No	Date	Arrival Time	Max.Amp.(M)	Group
118	20010201	07:06:57.40	4.94e-15	Group 1
119	20010201	22:55:06.99	3.15e-15	Group 1
120	20010203	02:37:35.70	1.83e-14	Group 2
121	20010204	11:04:41.00	1.41e-14	Group 2
122	20010206	01:29:09.95	7.23e-15	-
123	20010206	17:42:06.06	5.85e-15	-
124	20010207	14:15:44.05	1.01e-14	Gourp 2
125	20010207	21:17:36.98	5.37e-15	Group 1
126	20010210	16:45:30.62	5.02e-15	-
127	20010213	09:22:40.47	3.56e-15	Group 1
128	20010214	06:15:29.83	4.83e-15	Group 1
129	20010214	18:36:30.14	8.16e-15	Group 2
130	20010218	03:36:50.14	4.22e-15	Group 2
131	20010218	04:31:33.57	1.12e-14	Group 2
132	20010223	10:51:14.37	1.85e-15	Group 2
133	20010225	05:11:22.30	3.52e-15	Group 2
134	20010225	12:22:34.24	7.61e-15	Group 2
135	20010301	16:45:52.24	8.01e-15	Group 2
136	20010302	17:15:07.84	4.69e-15	Group 2
137	20010304	01:31:18.45	8.62e-15	Group 2

continued on next page

Table 2. *Continued*

No	Date	Arrival Time	Max.Amp.(M)	Group
138	20010305	06:34:34.86	7.46e-15	Group 2
139	20010306	03:45:09.12	5.55e-15	Group 2
140	20010307	09:00:39.98	5.42e-15	Group 2
141	20010308	04:00:34.31	4.63e-15	Group 2
142	20010308	23:28:17.04	3.65e-15	Group 2
143	20010309	11:23:29.92	3.37e-15	Group 2
144	20010316	05:30:41.34	3.78e-15	Group 2
145	20010405	20:17:27.98	4.64e-15	Group 2
146	20010406	03:04:31.71	1.58e-15	-
147	20011224	02:25:11.98	1.30e-15	Group 2
148	20020104	09:50:16.67	2.34e-15	Group 2
149	20020109	14:43:38.48	2.46e-15	Group 2
150	20020127	07:37:51.53	1.61e-15	Group 2
151	20020203	10:10:36.32	1.04e-15	-
152	20020203	17:18:58.21	6.80e-16	-
153	20020217	20:02:07.70	1.69e-15	-
154	20020311	11:00:14.30	5.24e-15	Group 2
155	20020311	20:39:46.44	1.84e-15	-
156	20020312	07:28:24.90	4.81e-15	Group 2
157	20020312	02:28:03.44	2.77e-15	-

continued on next page

Table 2. *Continued*

No	Date	Arrival Time	Max.Amp.(M)	Group
158	20020313	18:39:10.04	1.89e-15	Group 2
159	20020314	01:42:47.03	2.45e-15	Group 2
160	20020317	21:44:04.68	4.05e-15	Group 1
161	20020318	04:01:21.21	6.88e-15	Group 2
162	20020328	04:22:14.46	4.34e-15	Group 1
163	20020329	13:40:11.33	1.94e-15	-
164	20020330	10:20:23.18	1.65e-15	-
165	20020330	13:24:12.12	3.38e-15	Group 1
166	20020401	07:01:58.78	5.27e-15	Group 2
167	20020401	08:32:02.16	5.79e-16	-
168	20020402	18:23:26.24	2.10e-15	-
169	20020406	17:43:44.68	1.03e-15	-
170	20020408	11:34:51.75	1.57e-15	-
171	20020408	18:50:58.91	1.16e-15	-
172	20020408	19:06:23.73	1.33e-14	Group 2
173	20020410	15:41:42.74	3.43e-15	Group 2
174	20020411	12:17:01.32	4.73e-15	Group 2
175	20020411	14:04:32.80	1.06e-15	-
176	20020412	07:02:54.55	6.49e-16	-
177	20020412	08:26:09.67	1.22e-15	-

continued on next page

Table 2. *Continued*

No	Date	Arrival Time	Max.Amp.(M)	Group
178	20020412	09:18:32.66	1.04e-15	-
179	20020412	22:18:33.04	1.40e-15	-
180	20020412	09:57:42.45	8.07e-16	-
181	20020413	10:52:22.26	1.17e-14	Group 2
182	20020413	19:36:49.32	2.05e-15	Group 1
183	20020417	03:45:26.09	1.86e-15	Group 2
184	20020417	07:49:27.80	1.38e-15	-
185	20020418	20:58:50.33	9.66e-16	-
186	20020419	05:38:54.87	2.44e-15	Group 2
187	20020419	16:15:13.67	7.10e-16	-
188	20020420	03:56:44.97	4.78e-15	Group 2
189	20020420	19:52:39.18	5.44e-16	-
190	20020421	01:35:49.61	4.27e-15	Group 2
191	20020422	01:35:33.41	5.14e-15	Group 2
192	20020422	18:23:50.58	5.73e-15	Group 3
193	20020423	12:53:42.41	4.89e-15	Group 2
194	20020424	04:51:44.45	3.79e-15	Group 2
195	20020425	01:12:59.77	9.08e-15	Group 2
196	20020426	04:47:06.37	1.63e-15	-
197	20020426	14:20:26.89	5.47e-15	Group 2

continued on next page

Table 2. *Continued*

No	Date	Arrival Time	Max.Amp.(M)	Group
198	20020429	06:10:50.80	8.65e-16	-
199	20020429	07:18:47.91	9.19e-16	-
200	20020429	10:51:06.20	1.31e-157	-
201	20020429	11:22:42.71	6.69e-16	-
202	20020430	00:54:38.29	8.54e-16	-
203	20020504	11:24:45.17	5.97e-16	-
204	20020504	19:10:40.56	8.11e-16	-
205	20020504	21:56:05.21	1.42e-15	-
206	20020505	18:08:15.66	5.28e-16	-
207	20020509	00:40:12.07	1.86e-15	Group 2
208	20020511	07:43:18.01	5.43e-16	-
209	20020511	18:16:33.45	2.00e-15	Group 2
210	20020513	04:44:52.36	1.90e-15	Group 1
211	20020513	09:26:36.87	1.52e-15	-
212	20020513	17:21:26.22	7.26e-16	-
213	20020514	03:09:49.50	1.57e-15	Group 2
214	20020518	17:02:27.62	1.80e-15	Group 2
215	20020519	20:23:59.74	1.29e-15	Group 2
216	20020520	12:21:07.30	1.38e-15	Group 2
217	20020522	11:39:33.27	3.53e-15	Group 2

continued on next page

Table 2. *Continued*

No	Date	Arrival Time	Max.Amp.(M)	Group
218	20020524	10:24:49.44	1.75e-15	Group 1
219	20020528	06:05:43.14	1.06e-15	Group 2
220	20020530	08:59:31.11	1.31e-15	Group 1
221	20020603	09:31:56.28	6.34e-16	-
222	20020605	06:44:12.22	3.56e-15	Group 1
223	20020606	20:26:28.84	1.65e-15	Group 1
224	20020608	11:14:56.05	2.16e-15	Group 1
225	20020608	15:51:21.58	1.42e-15	-
226	20020609	14:45:57.72	1.34e-15	-
227	20020610	03:18:23.03	1.02e-15	-
228	20020611	16:24:55.62	5.41e-16	-
229	20020611	17:55:17.18	6.18e-16	-
230	20020613	20:35:49.69	8.25e-16	Group 2
231	20020614	04:13:14.68	9.12e-16	-
232	20020615	05:54:07.20	2.90e-15	Group 2
233	20020615	09:30:40.61	4.53e-15	Group 1
234	20020615	09:30:40.61	4.53e-15	Group 1
235	20020616	12:45:56.65	2.19e-14	Group 3
236	20020617	12:00:57.63	1.96e-15	Group 2
237	20020622	15:28:38.88	3.34e-15	Group 2

continued on next page

Table 2. *Continued*

No	Date	Arrival Time	Max.Amp.(M)	Group
238	20020623	13:55:29.52	2.31e-15	Group 1
239	20020623	20:13:10.40	3.89e-15	Group 1
240	20020626	06:54:16.12	1.53e-15	Group 2
241	20020702	07:01:38.55	1.98e-15	Group 2
242	20020703	10:33:37.46	1.44e-15	-
243	20020703	16:23:49.83	1.48e-15	Group 2
244	20020704	06:33:12.73	7.73e-16	-
245	20020705	09:21:40.52	7.79e-14	Group 2
246	20020708	10:57:28.80	7.46e-16	-
247	20020711	00:47:50.67	2.26e-15	Group 2
248	20020816	02:11:20.07	2.56e-15	Group 2
249	20020816	03:18:22.86	6.19e-15	Group 2
250	20020819	07:21:52.72	1.26e-15	-
251	20020822	22:03:13.96	1.43e-15	-
252	20020903	00:43:25.99	3.96e-16	-
253	20020910	01:42:39.70	3.10e-16	-
254	20020910	07:34:42.65	2.99e-16	-
255	20020910	10:05:07.19	1.89e-16	-
256	20020919	03:41:07.24	4.82e-15	Group 2
257	20021001	01:45:09.62	5.09e-15	Group 2

A.2 Video Examples of Group 1 and Group 2

A.2.1 Group 1 (Positive first VLP onsets)

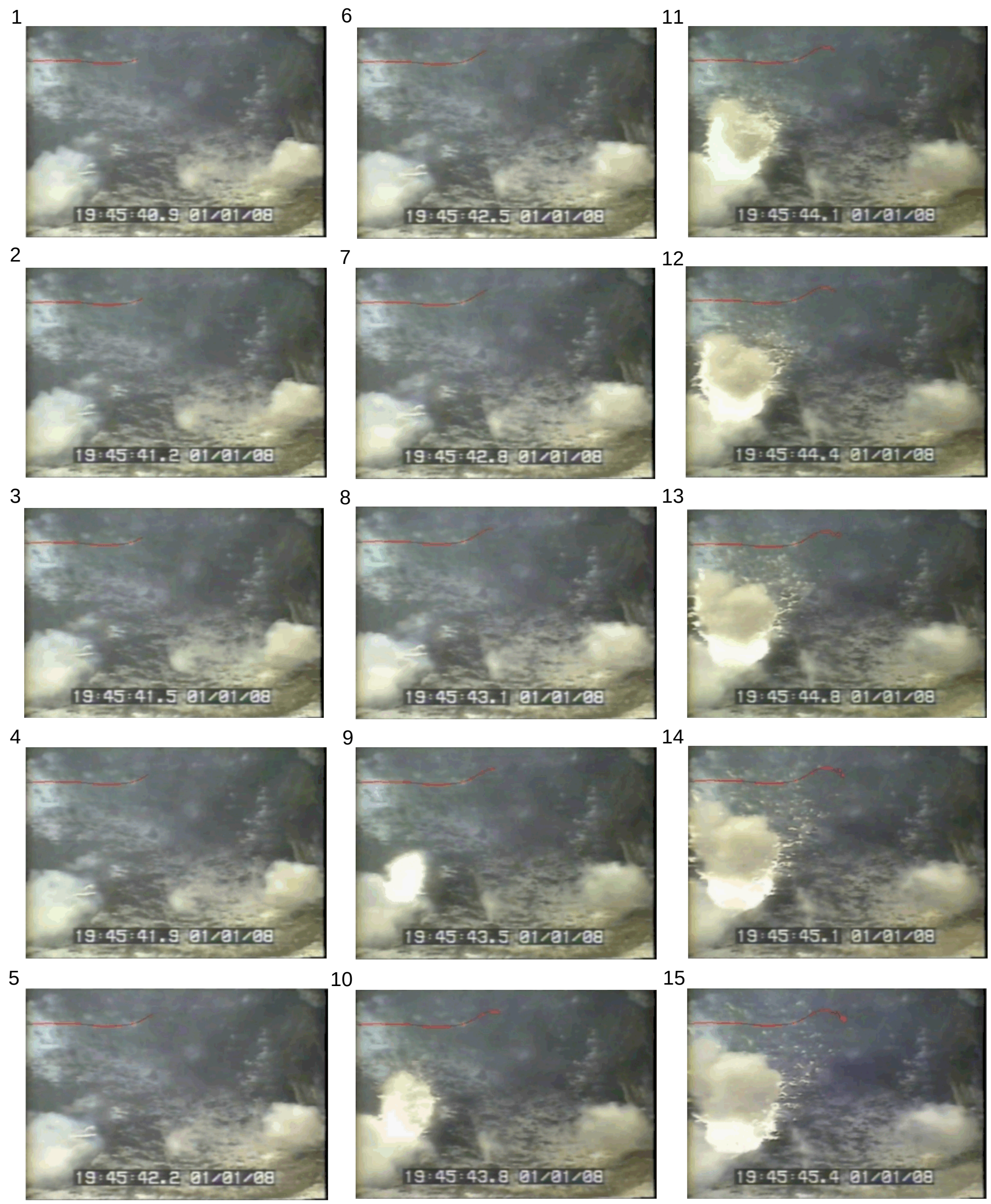

Figure A.2.1.a. Video example of a positive first VLP onset (Group 1) event. Video frames 9, 10, and 11 show a nearly vertical jet-like eruption style. VLP onset shows some time prior to lava lake surface activity (from frame 1 to 9).

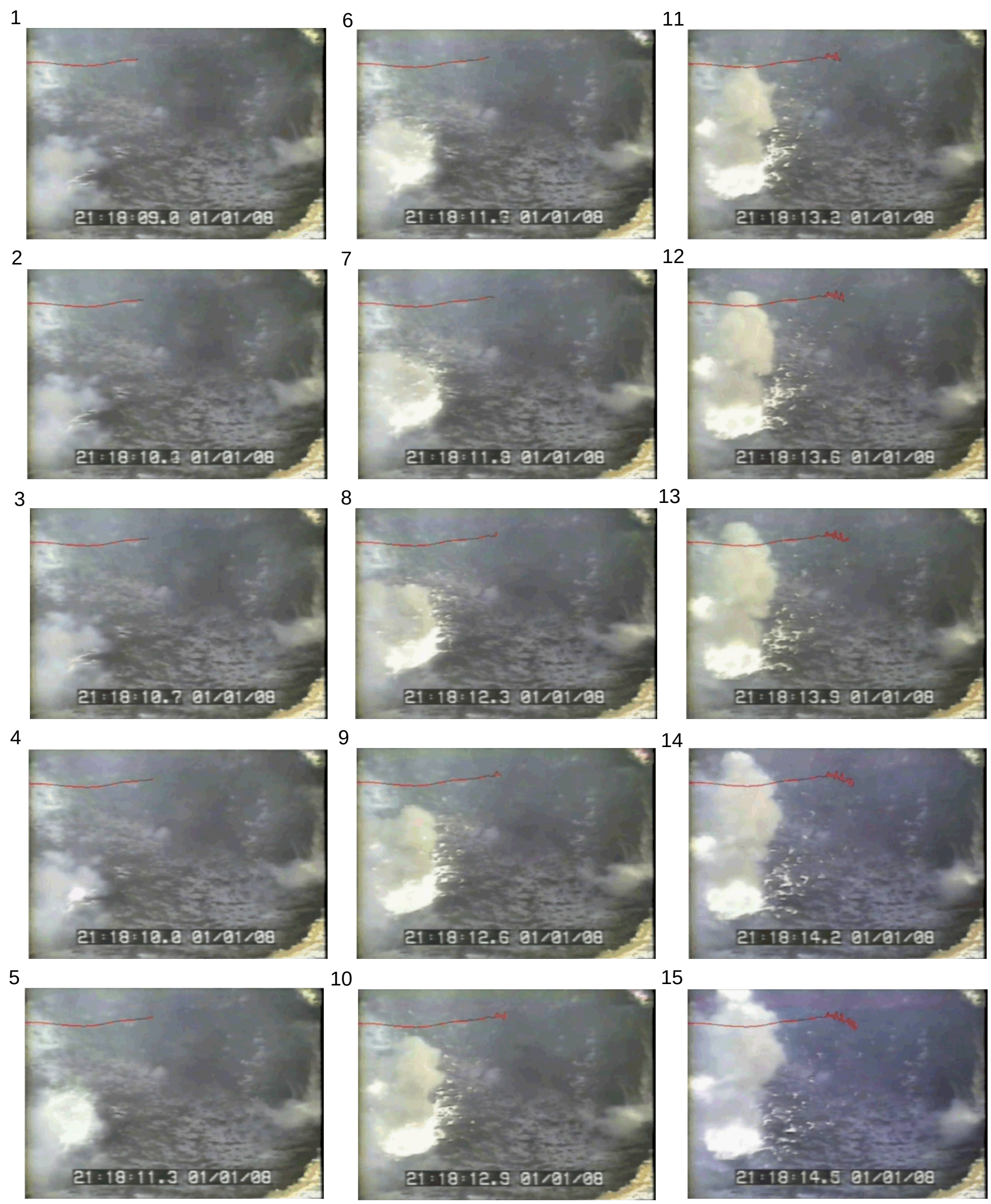

Figure A.2.1.b. Video example of a positive first VLP onset (Group 1) event. Video frames 5 show a nearly vertical jet-like eruption style. VLP onset shows some time prior to lava lake surface activity (from frame 1 to 4).

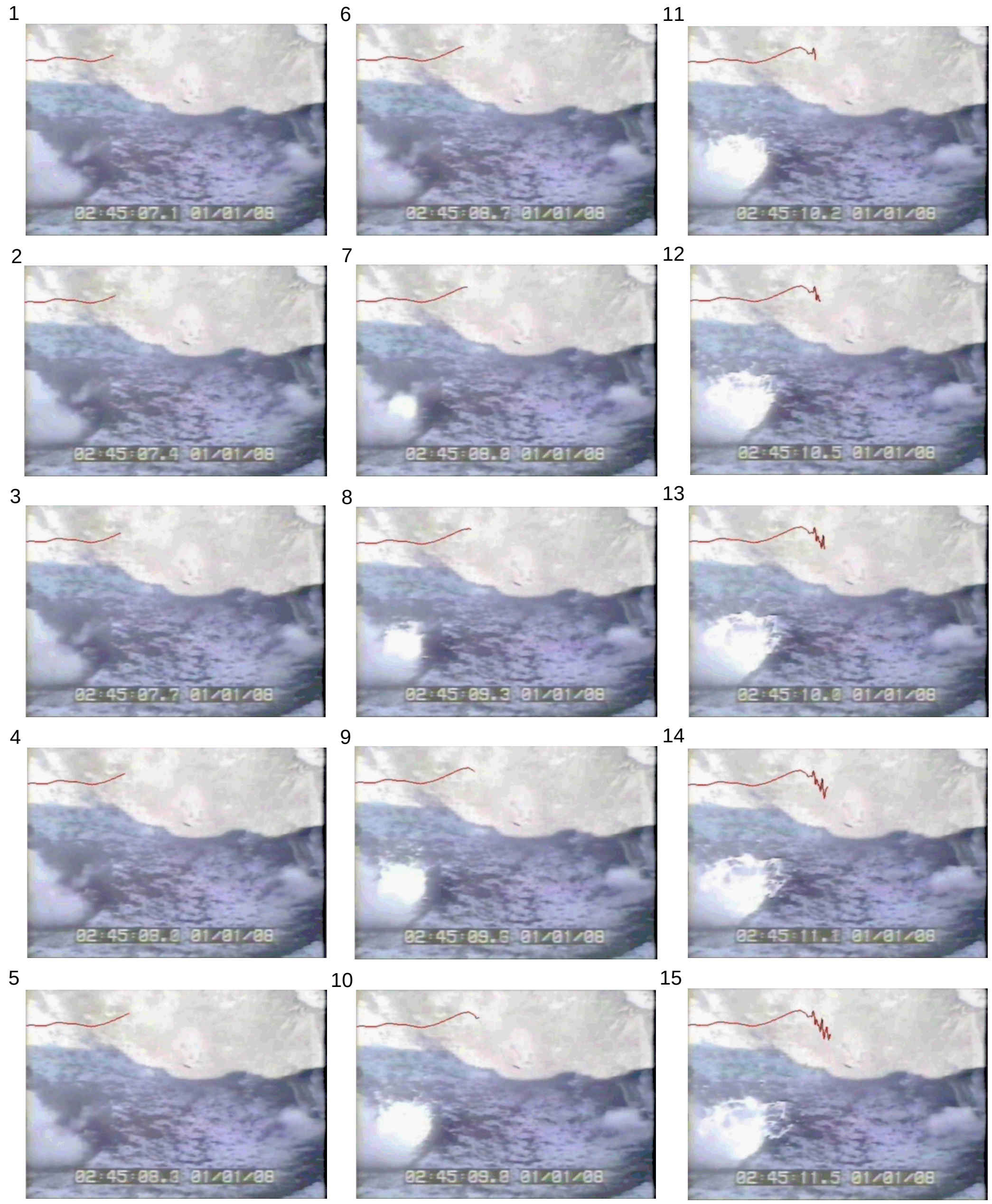

Figure A.2.1.c. Video example of a positive first VLP onset (Group 1) event. Video frames 7, 8, 9, and 10 show a nearly vertical jet-like eruption style. VLP onset shows some time prior to lava lake surface activity (from frame 1 to 6).

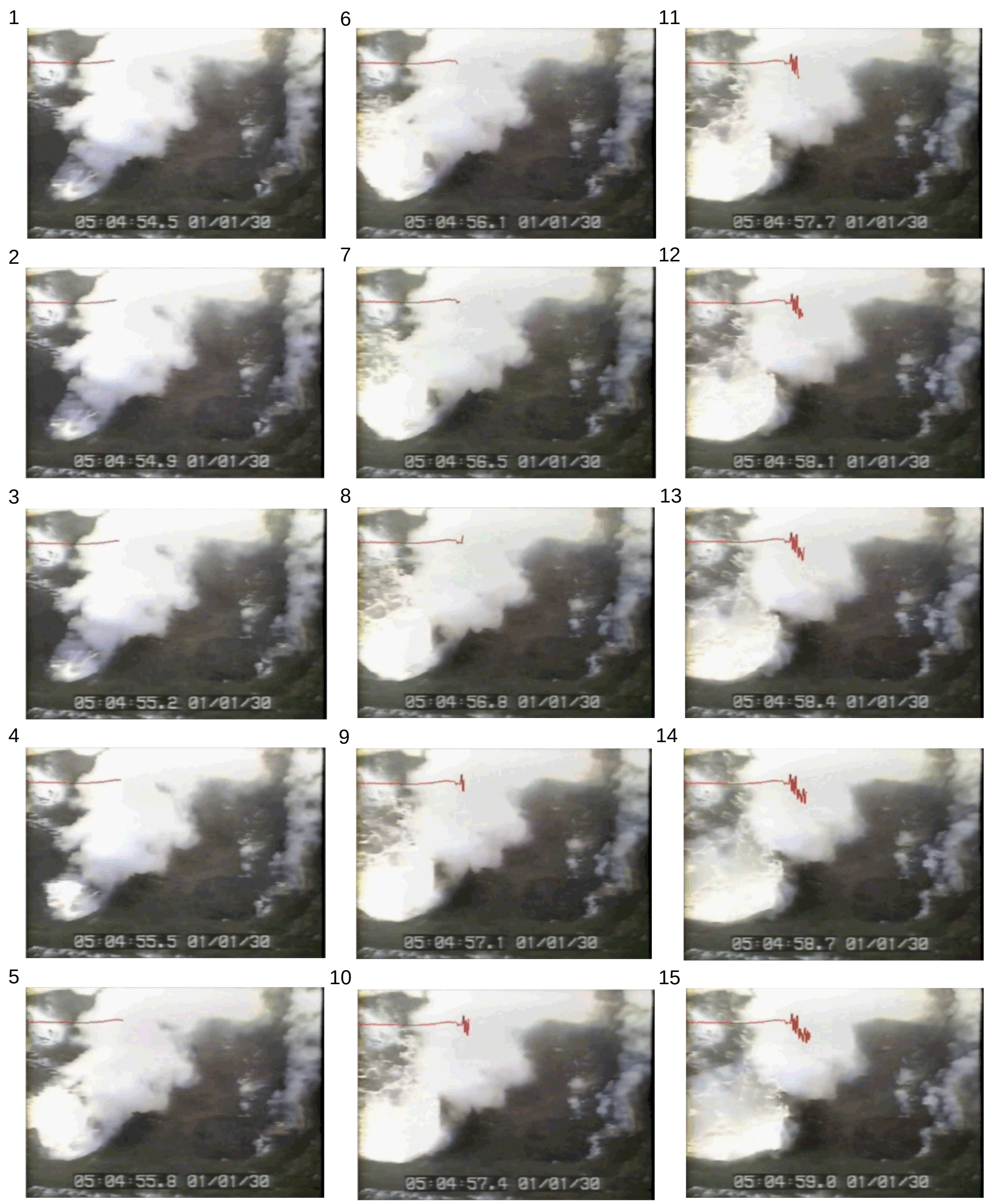

Figure A.2.1.d. Video example of a positive first VLP onset (Group 1) event. Video frames 4, 5, 6, 7, and 8 show a nearly vertical jet-like eruption style. VLP onset shows some time prior to lava lake surface activity (from frame 1 to 3).

A.2.2 Group 2 (Negative first VLP onsets)

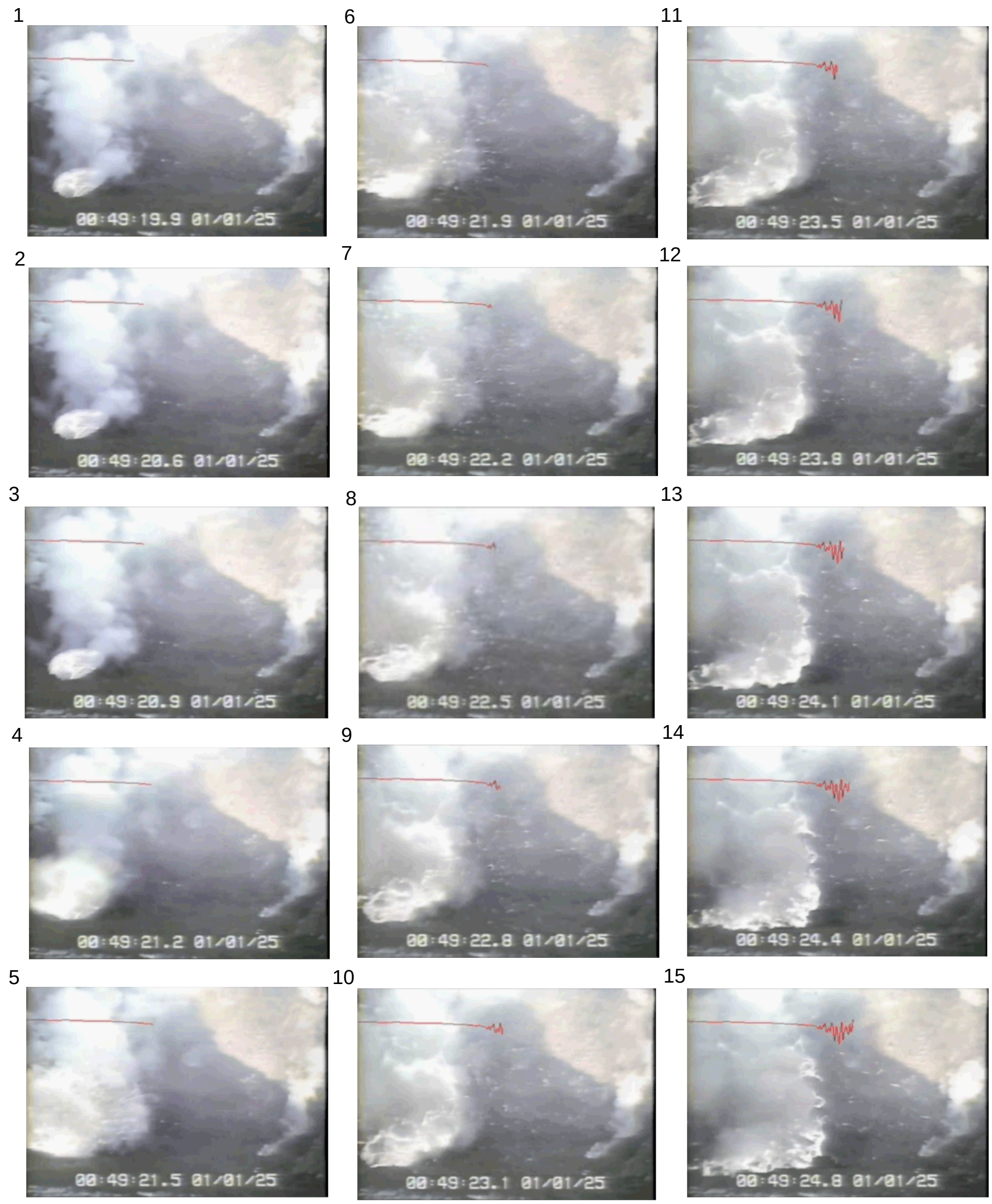

Figure A.2.2.a. Video example of a negative first VLP onset (Group 2) event. Video frames from 4 to 15 show a more radial eruption style. VLP onset shows some time prior to lava lake surface activity (from frame 1 to 3).

Figure A.2.2.b. Video example of a negative first VLP onset (Group 2) event. Video frames from 5 to 15 show a more radial eruption style. VLP onset shows some time prior to lava lake surface activity (from frame 1 to 4).

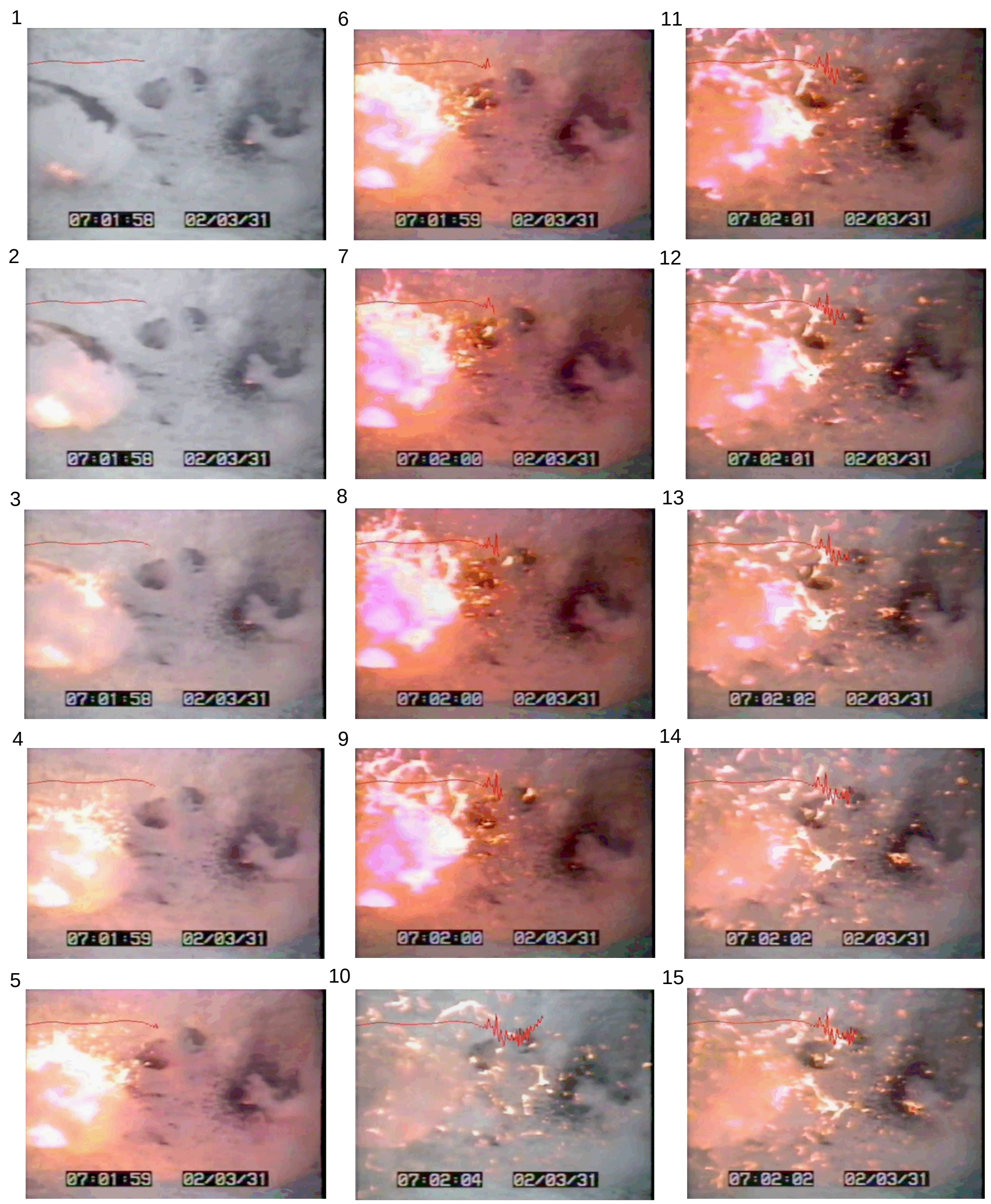

Figure A.2.2.c. Video example of a negative first VLP onset (Group 2) event. Video frames from 3 to 15 show a more radial eruption style. VLP onset shows some time prior to lava lake surface activity (from frame 1 to 2).

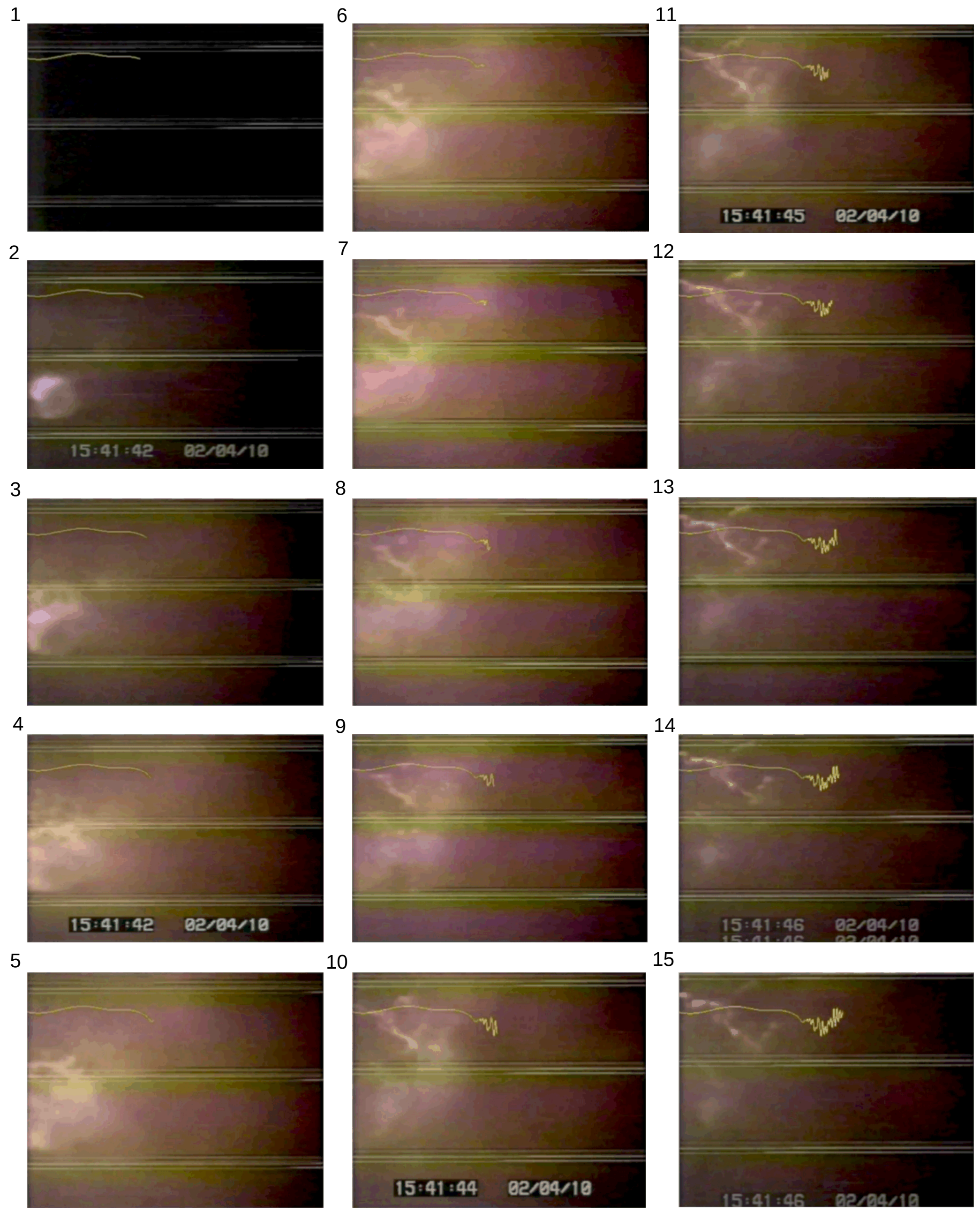

Figure A.2.2.d. Video example of a negative first VLP onset (Group 2) event. Video frames from 2 to 15 show a more radial eruption style. VLP onset shows some time prior to lava lake surface activity (frame 1).